# Assessment of wave runup and wave rundown based on observed long-term wave conditions

IOP Conf. Series: Materials Science and Engineering **700** (2019) 012006 doi:10.1088/1757-899X/700/1/012006

# Assessment of wave runup and wave rundown based on observed long-term wave conditions

**D Myrhaug* and T Sunde**

Dept. of Marine Technology, Norwegian University of Science and Technology, Trondheim, Norway

* Corresponding author: dag.myrhaug@ntnu.no

**Abstract**. The article presents an analytical method that can be applied to provide first estimates of wave runup (*RU*) and wave rundown (*RD*) on shorelines and coastal structures based on observed long-term wave statistics and is supplementary to [12] who based their results on long-term wind statistics. Some recently published wave *RU* and wave *RD* formulae are used, together with joint statistics of significant wave height and spectral peak period from the Northern North Sea. Results are exemplified for the average statistical properties of wave *RU* and wave *RD* in terms of the expected values and the standard deviations, as well as values estimated from 1-, 10- and 100-years return period contour lines.

## 1. Introduction

When waves approach a coastline, they usually break and run up on the coast, be it a structure or a beach. For low laying land or areas particularly exposed and vulnerable to waves this can represent critical situations leading to e.g. flooding, coastal erosion, and damage to coastal infrastructure such as breakwaters, seawalls, artificial reefs and sand barriers. Some recent works addressing these issues are those of [1], [2], [3] and [4]. The research attention has increased in the recent years driven by the focus on climate change and consequently possible sea level rise and more extreme weather. For shorelines and coastal structures, it is essential to reliably assess the maximum wave runup (*RU*) and the maximum wave rundown (*RD*) for safe design and cost-efficient coastal protections.

The wave *RU* height and the wave *RD* height are defined as the vertical difference between the highest and the lowest point, respectively, and the still water level. Two components contribute to the wave *RU*; the wave set-up and the swash. Here the wave set-up is the mean surface elevation level with reference to the mean surface elevation in deep water caused by the radiation stress (see [5]); the swash oscillates from the wave set-up corresponding to the interception between the water and the shoreline (or structure); see [1] for further details. Common design formulae for wave *RU* and wave *RD* use a 2% exceedance value of the *RU* maxima at the toe of the shoreline (or structure), $R_{2\%}$, as well as a 2% exceedance value of the *RD* maxima, $R_{d2\%}$. Most of these design formulae are given in terms of the surf (Iribarren) number, which is defined in terms of the significant wave height $H_s$ in deep water, the spectral peak period $T_p$ in deep water, and the slope of the shoreline (or the structure). Two other commonly used wave *RU* formulae are those of [6] and [7], where the first formula recently has been applied by [8]. However, these general formulae can not be treated by the present analytical approach.

Results from some recent studies will be advocated here and described briefly in Section 2; from [9], [1], [2], [3] and [4]. The latter reference gives a review and summary of wave *RU* formulae. Some of these recent wave *RU* formulae were applied by [10], [11] and [12] using long-term variation of wave and wind conditions. Here [10] and [11] based their results on long-term wave statistics, applying the wave *RU* formulae by [1] and the wave *RU* and wave *RD* formulae by [2], respectively. Further, [11] also demonstrated how 100-years return period values of wave *RU* and wave *RD* can be calculated based on a joint distribution of significant wave height and spectral surf parameter. The present article is supplementary to [12] who based their results on long-term wind statistics, applying eight wave *RU* formulae and one wave *RD* formula. The main purpose here is to demonstrate how similar and some additional results of wave *RU* and wave *RD* can be derived by using long-term wave statistics.

In this article it is demonstrated how long-term wave statistics in deep water can be applied to provide estimates of the wave *RU* and wave *RD* on shorelines or coastal structures. Results are obtained by adopting published formulae; eight wave *RU* and two *RD* formulae, together with a joint distribution of $H_s$ and $T_p$ from the Northern North Sea. A procedure of estimating the wave *RU* and wave *RD* from 1-, 10- and 100-years return period contour lines and the corresponding values of $H_s$, $T_p$ and the spectral surf parameter are also provided. The present analytical method should provide a useful tool that can be used for initial estimation of wave *RU* and wave *RD* in for instance early feasibility studies and risk analysis, or for estimations in the field.

## 2. Background

Extreme *RU* and *RD* events have been extensively investigated over the last decades in small- and large-scale laboratory studies as well as in field campaigns. The results are given in terms of empirical formulae representing estimates of the 2% exceedance values of *RU* and *RD* maxima. The formulae used in this article are adopted from some recently published works and are summarized in the following.

Two *RU* and one *RD* formulae were presented by [2]; the following two formulae for maximum wave *RU*

$$R_{2\%} = 1.165 H_s \xi_p^{0.77} \tag{1}$$

$$R_{2\%} = (0.39 + 0.795 \xi_p) H_s \tag{2}$$

and for maximum wave *RD*

$$R_{d2\%} = (0.21 - 0.44 \xi_p) H_s \tag{3}$$

Here $\xi_p$ is the spectral surf parameter defined as

$$\xi_p = m\left(\frac{H_s}{\frac{g}{2\pi} T_p^2}\right)^{-\frac{1}{2}} \tag{4}$$

where $m = \tan\alpha$ is the slope with an angle α with the horizontal, and *g* is the acceleration due to gravity. The wave *RU* formulae are based on the formulations by [13] and [14], with new empirical coefficients fitted to the equations; Equations (1) and (2) are modified versions of the original formulae by [13] and [14], respectively. Equations (1) to (3) were based on large-scale laboratory experiments on a prototype-scale sand barrier with a median grain size diameter $d_{50}$ = 0.42 mm, and are valid for *m* in the range 0.088 – 0.154 and $\xi_p$ in the range 1 – 2.9. Furthermore, [2] suggested that the linear model in $\xi_p$ (Eq. (2)) is the most easily applicable to *RU* data for the range of beach slopes they considered (see [2] for further details).

The following wave *RD* formulae based on data from a large-scale laboratory experiment was presented by [15]

$$R_{d2\%} = -0.1\xi_p^{2.21} H_s \tag{5}$$

The experiment was carried out using both the uniform slopes 1/6 and 1/12 and composite slopes with steepness 1/3 for the lower slope and 1/6 for the upper slope. For the composite slopes an appropriate average slope was calculated. The slope surface was covered by an asphalt concrete layer. This formula is based on data in the spectral wave steepness range $H_s/((g/2\pi)/T_p^2)$ of 0.001-0.031, and $0.5 < \xi_p < 2.5$.

The following wave *RU* model for $\xi_p < 0.6$, based on data from small-scale laboratory experiments for the three slopes 1/50, 1/30 and 1/20, and a sand seabed with $d_{50}$ = 0.7 mm was proposed by [1]

$$R_{2\%} = 4\,m^{0.3} H_s\,\xi_p \tag{6}$$

Assessment of wave *RU* predictions on beaches on the South-East Australian coast considering 11 existing empirical formulae was performed by [4]. The data used in this comparison represent sand bottom with $d_{50}$ in the range 0.25 – 0.5 mm, *m* in the range 0.02 – 0.16, $\xi_p$ in the range 0.32 – 1.65; the wave conditions in the assessment covered a range with average values of approximately $H_s = 1.5\,\mathrm{m}$ and $T_p = 8.9\,\mathrm{s}$, which are slightly below the typical mean conditions of the region of $H_s = 1.6\,\mathrm{m}$ and $T_p = 9.5\,\mathrm{s}$. However, the proposed models in Equations (9) and (10) are also considered to be valid for higher wave conditions because the formulae they are based on, cover a range up to $H_s = 5\,\mathrm{m}$ and $T_p = 15\,\mathrm{s}$. Among the 11 formulae [4] considered (in addition to Equations (9) and (10)) were those by [16] and [9]. The wave *RU* formula by [16] is given as

$$R_{2\%} = (0.2 + 0.83\xi_p) H_s \tag{7}$$

and based on data from measurements at Duck, North Carolina, USA.

The wave *RU* formula by [9] is given as

$$R_{2\%} = (0.58\,m + 0.53\xi_p) H_s + 0.45 \tag{8}$$

and based on field measurements on the south coast of Algarve, Portugal representing the European Atlantic coast. The data they used were based on manually selected wave *RU* maxima representing *m* in the range 0.04 - 0.15, $\xi_p$ in the range 0.3 – 2.9, sand seabed with $d_{50}$ = 0.50 mm.

The formulae by [4] are

$$M1\ R_{2\%} = 0.99\,H_s\,\xi_p \tag{9}$$

$$M2\ R_{2\%} = (0.16 + 0.92\,\xi_p) H_s \tag{10}$$

and are based on the best fit to the 11 formulae they considered, where the one in Equation (9) is forced through the origin (i.e. with the origin in $\xi_p$ = 0 for $R_{2\%}/H_s$ versus $\xi_p$).

Moreover, [3] proposed a parameterization of wave *RU* from field measurements on gravel beaches and numerical calculation given as

$$R_{2\%} = C\,m^{0.5}\,T_p\,H_s\ ;\ C = 0.33 \tag{11}$$

The field data they used were obtained during a 2-year period including storm conditions with $H_s$ in the range 1 – 8 m, *m* in the range 0.05 – 0.20, $\xi_p$ in the range 0.2 -1.9, $d_{50}$ in the range 2 -50 mm (see [3] for more details).

As a summary, Equations (1) to (3) and (5) to (10) can be represented as

$$R_2 = a\,H_s + b\,H_s\,\xi_p^c + d \tag{12}$$

**Table 1.** Wave *RU* and *RD* formulae according to Equation (12) for models 1 to 9 and Equation (11) for model 10.

| Model nr | Abbreviation | Ref. | a | b | c | d | C |
|---|---|---|---|---|---|---|---|
| | | [2] | | | | | |
| 1, RU | Bl 1 | | 0 | 1.165 | 0.77 | 0 | - |
| 2, RU | Bl 2 | | 0.39 | 0.795 | 1 | 0 | - |
| 3, RD | Bl d | | 0.21 | -0.44 | 1 | 0 | - |
| 4, RD | Sc | [15] | 0 | -0.1 | 2.21 | 0 | - |
| 5, RU | Pe | [1] | 0 | 4m0.3 | 1 | 0 | - |
| 6, RU | Ho | [16] | 0.2 | 0.83 | 1 | 0 | - |
| 7, RU | Vo | [9] | 0.58m | 0.53 | 1 | 0.45 | - |
| | | [4] | | | | | |
| 8, RU | At1 | | 0 | 0.99 | 1 | 0 | - |
| 9, RU | At2 | | 0.16 | 0.92 | 1 | 0 | - |
| 10, RU | Po | [3] | - | - | - | - | 0.3<br>3 |

where $R_2$ represents $R_{2\%}$ for wave *RU* and $R_{d2\%}$ for wave *RD*, and the coefficients *a, b, c, d* are given in Table 1.

As referred to in Section 1, the wave *RU* formulae by [6] and [7] are frequently used for assessing wave *RU*, but can not be treated analytically. In particular, the formulations by [7] cover a wide range of conditions on different slopes on shallow and very shallow foreshores with different surface roughnesses, although some of the formulae, e.g. their Equations (5.1), (5.2), (5.5) and (5.6) have the forms of Equation (12). Alternative methods are, for instance; to apply Monte Carlo simulations, or simple methods as those of [17] or [18].

Thus, according to Equations (11) and (12), $R_2$ is given in terms of the deep water sea state parameters $H_s$ and $T_p$. Different parametric models for the joint probability density function (*pdf*) of $H_s$ and $T_p$ are available in the literature; see [19] for a review. The joint *pdf* used to exemplify the results in this article is taken from [20], given as

$$p(H_s,T_p) = p(T_p \mid H_s)p(H_s) \tag{13}$$

Here $p(H_s)$ is the marginal *pdf* of $H_s$, given by the following combined lognormal and Weibull distributions

$$p(H_s) = \begin{Bmatrix} \dfrac{1}{\sqrt{2\pi}\kappa H_s}\exp\left[-\dfrac{(ln\,H_s-\theta)^2}{2\kappa^2}\right], H_s \le 3.25\,\mathrm{m} \\ \beta\dfrac{H_s^{\beta-1}}{\zeta^{\beta}}\exp\left[-(\dfrac{H_s}{\zeta})^{\beta}\right], H_s > 3.25\,\mathrm{m} \end{Bmatrix} \tag{14}$$

where $\theta = 0.801$, $\kappa^2 = 0.371$ are the mean value and the variance, respectively, of $ln\,H_s$ and $\zeta = 2.713$, $\beta = 1.531$ are the Weibull parameters.

$p(T_p \mid H_s)$ is the conditional *pdf* of $T_p$ given $H_s$, given by the lognormal *pdf*

$$p(T_p \mid H_s) = \frac{1}{\sqrt{2\pi}\sigma T_p}\exp\left[-\frac{(ln\,T_p-\mu)^2}{2\sigma^2}\right] \tag{15}$$

where $\mu$ and $\sigma^2$ are the mean value and the variance, respectively, of $ln\,T_p$ given as

$$\mu = a_1 + a_2\, H_s^{a_3}\ ,\ (a_1, a_2, a_3) = (1.780, 0.288, 0.474) \tag{16}$$

$$\sigma^2 = b_1 + b_2\, e^{b_3 H_s}, (b_1, b_2, b_3) = (0.001, 0.097, -0.255) \tag{17}$$

This joint *pdf* of $H_s$ and $T_p$ was obtained as a best fit to 29 years of wave data from the Northern North Sea representing wind waves, swell waves and combinations; see [20] for more details. The unit of $H_s$ in Equations (16) and (17) is in meter.

It should be noted that the wave *RU* and wave *RD* formulae used here are based on data from other locations than the wave data. Therefore, in a proper analysis the wave data should be from the same location as the wave *RU* and wave *RD* models are based on. However, here the present wave data are used since the main purpose is to demonstrate the application of the method.

## 3. Statistical properties of *RU* and *RD*

The statistical properties of $R_2$, from which the statistical properties of $R_{2\%}$ and $R_{d2\%}$ follow, are derived from the joint *pdf* of $H_s$ and $T_p$, giving the joint *pdf* of $R_2$ and $H_s$. This is achieved from Equations (11) and (12) by a change of variables from $(H_s, T_p)$ to $(H_s, R_2)$, yielding

$$p(H_s, R_2) = p(R_2 \mid H_s)\, p(H_s) \tag{18}$$

From Equations (11), (4), (12) and (13) it is noticed that this change of variables only affects $p(T_p \mid H_s)$.

First, consider Equations (4) and (12) from which

$$T_p = \left[ \frac{R_2 - aH_s - d}{bm^c \left( \dfrac{g}{2\pi} \right)^{\frac{c}{2}} H_s^{1-\frac{c}{2}}} \right]^{\frac{1}{c}} \tag{19}$$

This gives the Jacobian

$$\left| \frac{\partial T_p}{\partial R_2} \right| = \frac{\dfrac{1}{c} (R_2 - aH_s - d)^{\frac{1}{c}-1}}{\left[ bm^c (\dfrac{g}{2\pi})^{\frac{c}{2}} H_s^{1-\frac{c}{2}} \right]^{\frac{1}{c}}} \tag{20}$$

Thus, by using this Jacobian and that $p(R_2 \mid H_s) = p(T_p \mid H_s) \mid \partial T_p / \partial R_2 \mid$, the following lognormal *pdf* of $R_2$ given $H_s$ is obtained

$$p(R \mid H_s) = \frac{1}{\sqrt{2\pi}\, \sigma_R R} \exp\left[ -\frac{(lnR - \mu_R)^2}{2\sigma_R^2} \right] \tag{21}$$

where

$$R = R_2 - aH_s - d \tag{22}$$

and $\mu_R$ and $\sigma_R^2$ are the conditional mean value and conditional variance, respectively, of $ln\, R$, given as

$$\mu_R = c\mu + ln[bm^c (\frac{g}{2\pi})^{\frac{c}{2}} H_s^{1-\frac{c}{2}}] \tag{23}$$

$$\sigma_R^2 = (c\ \sigma)^2 \tag{24}$$

where $\mu$ and $\sigma^2$ are given in Equations (16) and (17), respectively.

The conditional cumulative distribution function (*cdf*) of $R$ given $H_s$ is given by the standard Gaussian *cdf* $\Phi$ as ([21])

$$P(R \mid H_s) = \Phi\left[\frac{ln\,R - \mu_R}{\sigma_R}\right] \tag{25}$$

$$\Phi(v) = \frac{1}{\sqrt{2\pi}} \int_{-\infty}^{v} e^{-t^2/2} dt \tag{26}$$

Then, the expected value and the standard deviation of R given $H_s$ are given in Equations (27) and (28), respectively, as ([21])

$$E\left[R \mid H_s\right] = \exp(\mu_R + \frac{1}{2}\sigma_R^2) \tag{27}$$

$$\sigma\left[R \mid H_s\right] = \left[(e^{\sigma_R^2} - 1)\exp(2\mu_R + \sigma_R^2)\right]^{1/2} \tag{28}$$

Thus, from Equation (22) it follows that

$$E\left[R_2 \mid H_s\right] = E\left[R \mid H_s\right] + aH_s + d \tag{29}$$

$$\sigma\left[R_2 \mid H_s\right] = \sigma\left[R \mid H_s\right] \tag{30}$$

Similarly, by taking Equation (11) as $R_2 = C\,m^{0.5}\,H_s\,T_p$, a change of variables from $(H_s, T_p)$ to $(H_s, R_2)$ only affects $p(T_p \mid H_s)$. Then, by using the Jacobian $|\partial T_p / \partial R_2| = 1/(C\ m^{0.5}\ H_s)$, this yields a lognormal *pdf* of $R_2$ given $H_s$ in the form

$$p(R_2 \mid H_s) = \frac{1}{\sqrt{2\pi}\sigma_{R_2} R_2} \exp\left[-\frac{(ln\,R_2 - \mu_{R_2})^2}{2\sigma_{R_2}^2}\right] \tag{31}$$

where the conditional mean value and the conditional variance, respectively, of $ln\,R_2$, are given as

$$\mu_{R_2} = \mu + ln(C\ \ m^{0.5}\ H_s) \tag{32}$$

$$\sigma_{R_2}^2 = \sigma^2 \tag{33}$$

where $\mu$ and $\sigma^2$ are given in Equations (16) and (17), respectively.

## 4. Example of results

### 4.1. Conditional statistical values of RU and RD within a sea state

Here the average statistical properties of *RU* and *RD* expressed in terms of the expected values and the standard deviations are provided. Examples of results are given for

- Significant wave height in deep water, $H_s = 3\,\mathrm{m}$
- Slope, $m = 1/10$

These parameters are within the validity range of the models (except for model 5 which is valid for $m = 1/50,\ 1/30,\ 1/20$ ), and is used here to serve the purpose of demonstrating the application of the method.

**Table 2.** Conditional expected values of *RU* for models 1, 2, 5 to 10 and *RD* for models 3, 4, for $H_s = 3\,\mathrm{m}$ and slope $m = 1/10$ (column 3); the corresponding expected value (EV) $\pm 1$ standard deviation (SD) (column 4); see also Table 1.

| Model nr | Abbreviation | EV (m) | EV $\pm 1$ SD (m) |
|---|---|---|---|
| 1, RU | Bl 1, Eq. (1) | 2.7 | 2.2, 3.1 |
| 2, RU | Bl 2, Eq. (2) | 2.9 | 2.5, 3.2 |
| 3, RD | Bl d, Eq. (3) | -0.31 | -0.51, -0.10 |
| 4, RD | Sc, Eq. (5) | -0.15 | -0.23, -0.07 |
| 5, RU | Pe, Eq. (6) | 4.3 | 3.3, 5.2 |
| 6, RU | Ho, Eq. (7) | 2.4 | 2.0, 2.8 |
| 7, RU | Vo, Eq. (8) | 1.8 | 1.5, 2.0 |
| 8, RU | At 1, Eq. (9) | 2.1 | 1.7, 2.6 |
| 9, RU | At 2, Eq. (10) | 2.4 | 2.0, 2.9 |
| 10, RU | Po, Eq. (11) | 3.1 | 2.4, 3.8 |

For these conditions the expected value (EV) and the expected value plus and minus one standard deviation (SD), i.e. $\mathrm{EV} \pm 1\,\mathrm{SD}$, of *RU* and *RD* can be calculated. The results are given in Table 2 showing that EV for wave *RU* ranges from 1.8m to 4.3m, with the lowest value based on model 7 and the highest value based on model 5; the coefficient of variation (SD/EV) varies from about 0.1 to about 0.2 with the lowest value for model 2 and the highest for model 5. Furthermore, EV for wave *RD* are -0.31m and -0.15m for models 3 and 4, respectively, while SD/EV is about 0.05 and 0.5, respectively. Based on the results for $\mathrm{EV} \pm 1\,\mathrm{SD}$ it appears that there is overlap between the values obtained by the two wave *RD* models 3 and 4, suggesting that the results are consistent. For the values obtained by the eight wave *RU* models there is overlap between models 1, 2, 6, 8, 9, 10; between models 7 and 8; between models 5 and 10. It should also be noted that the $\mathrm{EV} + 1\,\mathrm{SD}$ value of model 7 coincides with the EV – 1 SD values of models 6 and 9. Overall, this suggests that the results from models 1, 2, 6, 8, 9, 10 are consistent. It should be recalled that these results are not general, but valid for $H_s = 3\,\mathrm{m}$ and the slope $m = 1/10$ (which is outside the validity range of model 5 and thus the result for this model is less reliable). Moreover, these results are associated with the present $p(H_s, T_p)$, and thus other joint *pdfs* from the same locations as the wave *RU* and wave *RD* models are based might give different results.

*4.2. Estimation of RU and RD from n-years return period contour lines of* $p(H_s, T_p)$

N-years return period values of *RU* and *RD* can be estimated from the n-years return period contour lines of $p(H_s, R_2)$ in Equation (19). However, an alternative is to estimate these values of *RU* and *RD* from the n-years return period contour lines of $p(H_s, T_p)$ in Equations (13) to (17).

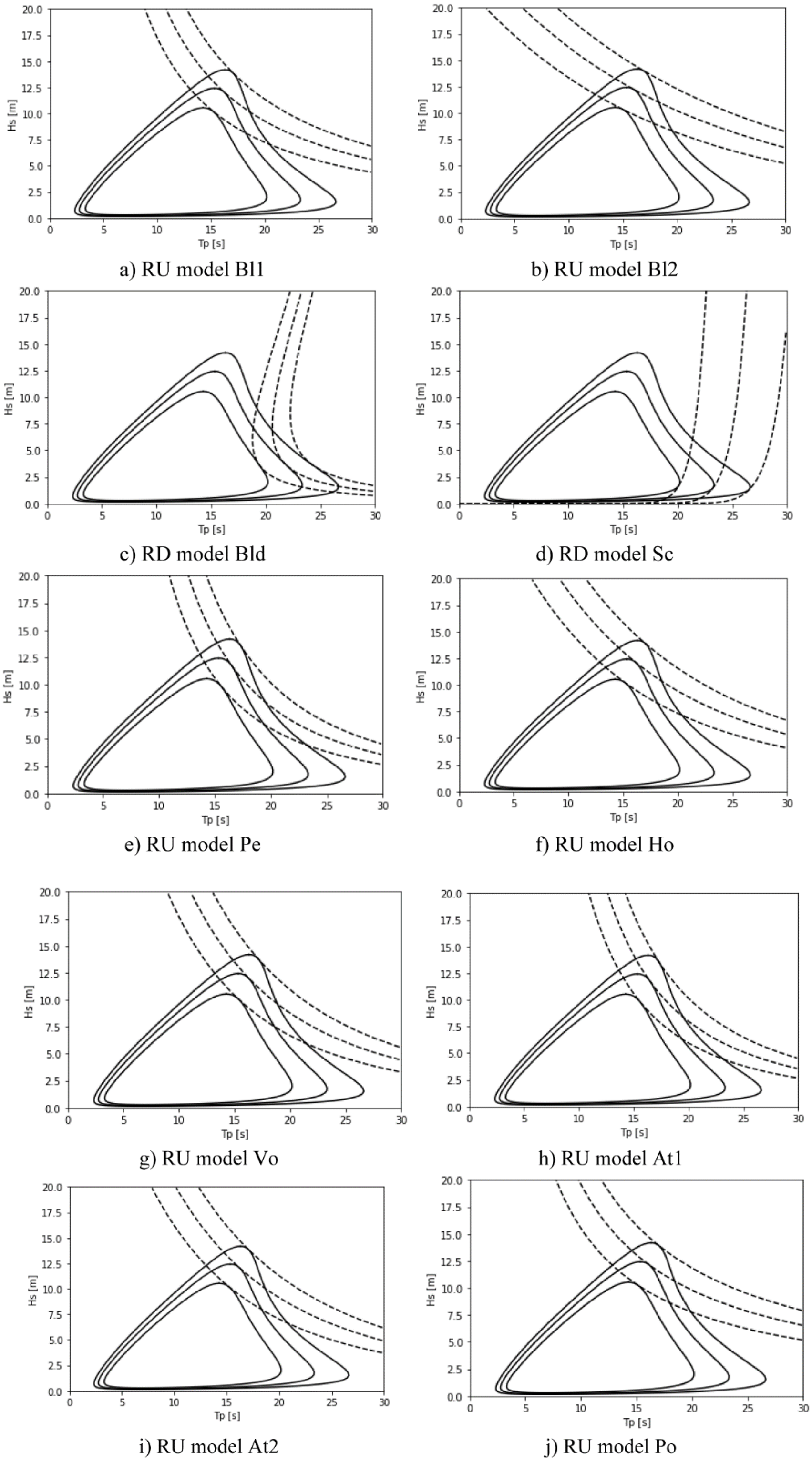


**Figure 1.** 1-year, 10-years and 100-years contour lines of $H_s$ (m) (vertical axes) and $T_p$ (s) (horizontal axes) from the inner to outer contours, respectively, with the tangent lines corresponding to: (a) *RU* model 1; (b) *RU* model 2; (c) *RD* model 3; (d) *RD* model 4; (e) *RU* model 5; (f) *RU* model 6; (g) *RU* model 7; (h) *RU* model 8; (i) *RU* model 9; (j) *RU* model 10. See also Tables 1 and 3.

Figure 1 depicts the 1-year, 10-years and 100-years return period contour lines by assuming a sea state duration of 3 hours, represented by the inner to the outer contours, respectively, obtained using the IFORM method described in [22]. This method is based on transformation of the joint *cdf* of $H_s$ and $T_p$ to the standard Gaussian *cdf*, from which the return period contour lines are determined as circles.

First, consider Equation (11) which by solving for $H_s$ gives

$$H_s = \frac{R_2}{C\, m^{0.5}}\, T_p^{-1} \tag{34}$$

For a given value of $R_2$, this is a curve in the $(H_s, T_p)$ plane. The values of $R_2$ which implies that these curves will have tangent points with the 1-year, the 10-years and the 100-years contours can be determined by iteration, and thus the corresponding tangent points. The results are shown graphically in Figure 1j by the three curves giving tangent points to the 1-, 10-, 100-years contours for $R_2$ = 16.2 m, 20.5 m and 24.7 m respectively, corresponding to the 1-, 10-, 100-years return period values of $R_2$ based on model 10 and the slope $m = 1/10$. However, how realistic these large values of $R_2$ are, is questionable; more discussion is given subsequently. It is observed that these values of $R_2$ are governed by $H_s$ in the sense that the tangent points are located close to the maximum values of $H_s$ along the respective return period contours. The corresponding coordinates of the tangent points for $H_s, T_p$ are given in Table 3, together with the corresponding values of $\xi_p$ according to Equation (4).

Second, consider Equation (12), which for a given value of $R_2$ represents a curve in the $(H_s, T_p)$ plane. Also in this case the values of $R_2$ corresponding to the tangent points to the 1-, 10-, 100-years contours are found by iteration. The results are shown graphically in Figures 1a, b, e – i for *RU* and in Figures 1c, d for *RD* by the three curves giving tangent points to the 1-, 10-, 100-years contours. The values of $R_2$ and the corresponding values of $H_s, T_p$ and $\xi_p$ for each of the *RU* and *RD* models are given in Table 3 for the slope $m = 1/10$. It is observed that these values of $R_2$ corresponding to *RU* are governed by $H_s$. However, the values of $R_2$ corresponding *RD* (Figures 1c, d) are related to tangent points given by combined lower $H_s$ and higher $T_p$ values.

**Table 3.** Extreme values of *RU* $(R_2)$ for models 1, 2, 5 to 10 and *RD* $(R_2)$ for models 3, 4 corresponding to the 1- 10, 100-years contours of $(H_s, T_p)$ and corresponding values of $H_s$, $T_p$, $\xi_p$ (for the slope $m = 1/10$), from left to right for each variable, respectively; see also Table 1.

| Model nr | $R_2$ (m) | $H_s$ (m) | $T_p$ (s) | $\xi_p$ |
|---|---|---|---|---|
| 1, RU | 8.0, 9.3, 10.5 | 10.2, 12.0, 13.9 | 15.2, 16.3, 17.0 | 0.60, 0.59, 0.57 |
| 2, RU | 8.8, 10.3, 11.7 | 10.3, 12.3, 14.1 | 15.0, 15.9, 16.8 | 0.58, 0.56, 0.56 |
| 3, RD | -1.3, -1.5, -1.8 | 3.6, 3.4, 3.6 | 19.4, 22.1, 24.4 | 1.3, 1.5, 1.6 |
| 4, RD | -0.72, -1.0, -1.4 | 1.7, 1.6, 1.3 | 20.1, 23.3, 26.5 | 2.0, 2.3, 2.9 |
| 5, RU | 12.2, 14.2, 16.0 | 9.8, 11.8, 13.7 | 15.6, 16.5, 17.2 | 0.62, 0.60, 0.58 |
| 6, RU | 7.1, 8.3, 9.4 | 10.2, 12.2, 13.9 | 15.2, 16.1, 17.0 | 0.60, 0.58, 0.57 |
| 7, RU | 4.3, 4.9, 5.5 | 10.0, 12.0, 13.7 | 15.4, 16.3, 17.2 | 0.61, 0.59, 0.58 |
| 8, RU | 6.0, 7.0, 7.9 | 9.8, 11.8, 13.7 | 15.6, 16.5, 17.2 | 0.62, 0.60, 0.58 |
| 9, RU | 7.2, 8.4, 9.5 | 10.2, 12.0, 13.9 | 15.2, 16.3, 17.0 | 0.60, 0.59, 0.57 |
| 10, RU | 16.2, 20.5, 24.7 | 10.3, 12.2, 13.9 | 15.0, 16.1, 17.0 | 0.58, 0.58, 0.57 |

It should be noted that some of the estimated *RU* and *RD* values are obtained by exceeding the surf parameter validity bounds stated in Section 2, but is used here with the purpose of demonstrating the application of the method. This is the case for models 1 and 2 for all predictions, since the models are valid for $\xi_p$ in the range 1 to 2.9; for model 4 for the 100-years return period value since $\xi_p = 2.9 > 2.5$; for model 5 for the 1-year return period value since $\xi_p = 0.62 > 0.6$. Furthermore, it is also noticed that the *RU* values from models 5 and 10 are large compared to the other model predictions. As referred to earlier, model 5 is valid for smaller slopes than $m = 1/10$ used here, and thus the results for this model are less reliable. If a smaller slope (i.e. in the range 1/50-1/20) is applied for the same wave conditions, it is expected to predict lower *RU* values (see Equation (6)). The model 10 results should be reasonable since Equation (11) is used within its range of validity. However, a firm statement on the validity of the return period results is not possible without comparison with measurements.

A similar procedure can be applied for other joint distributions of $H_s, T_p$ as well as for other $n$ – years return period contour lines to obtain the wave *RU* and wave *RD* values and the corresponding values of $H_s, T_p$ and $\xi_p$. However, as mentioned in Section 2, the wave data should be from the same location as the wave *RU* and wave *RD* models are based on.

### *4.3. Discussion*
This section provides some comments on this approach versus a procedure which applies more complete computational demanding methods without using empirical formulae. For assessing the maximum wave *RU* and wave *RD* heights, common practice would be to start with available data on joint statistics of $H_s$ and $T_p$ (or other characteristic wave periods); preferably within directional sectors at a nearby location offshore (in deep water). The next step would be to apply a wave simulation model that includes effects of dissipation due to bottom friction and wave breaking, and thereby to obtain the joint statistics of $H_s$ and $T_p$ at the coastal (shallow water) site; then finally to use this as input for computing the maximum wave *RU* and wave *RD* heights. In general this practice would also include sites exposed to sea states with combined wind waves and swell waves from different directions. In this article an alternative is presented providing an analytical method which can be used to estimate maximum wave *RU* and wave *RD* heights from given deep water values of $H_s$ and $T_p$, exemplified by including results using a joint distribution of $H_s$ and $T_p$ representing wind waves, swell waves and combinations.

The transition from deep water to the coastal site is assumed to be smooth, i.e. by neglecting wave energy dissipation effects over changing bed conditions with varying intermediate and shallow water depths. As a result, several effects affecting the estimated wave *RU* and wave *RD* heights are neglected, e.g.: that the wave field is inhomogeneous; from where the waves are coming and the location of the assessment site; return flows from dissipation effects which in turn will affect the local wave conditions. However, the approach enables analytical estimates of the maximum wave *RU* and wave *RD* heights, which are appropriate for making quick estimates. Then, these estimates can be used to compare with more complete computationally demanding methods. Under field conditions such an easily accessible and simple tool might also be useful as there is usually limited time and access to computational resources. Although the presented results are based on specific wave *RU* and wave *RD* formulae and a joint $(H_s, T_p)$ distribution from another location than the wave *RU* and wave *RD* models are based on, the method can also be applied for other wave *RU* and wave *RD* formulae that can be treated analytically, joint distributions of sea state wave parameters, or for a given deep water wave spectrum including directional spreading effects. However, in such cases numerical calculations are most probably required. It is important, however, to assess the accuracy of this simple approach versus common practice, which is only possible to quantify by comparing with such methods over a wide parameter range, also including a sensitivity analysis of the results regarding the assumptions considered, but this is beyond the scope of this article.

## 5. Conclusions

An analytical method that can be applied to provide estimates of wave *RU* and wave *RD* on shorelines and coastal structures is presented. Results are achieved by adopting eight wave *RU* formulae and two wave *RD* formulae together with observed long-term wave statistics from deep water in the Northern North Sea. Expected values and variances of the 2% exceedance values of the wave *RU* maxima and the wave *RD* maxima are calculated. The main purpose is to demonstrate how long-term wave statistics can be used to obtain first estimates of wave *RU* and wave *RD*.

Examples of results for typical realistic conditions are also provided by presenting the conditional expected value (EV) plus and minus one standard deviation (1 SD) of the 2% exceedance values of the wave *RU* maxima and the wave *RD* maxima within a sea state. By comparing the results from the eight wave *RU* models and the corresponding $\mathrm{EV} \pm 1\ \mathrm{SD}$, it is overlap between models 1, 2, 6, 8, 9, 10; between models 7 and 8; between models 5 and 10; as well as between the two *RD* models 3 and 4. Overall, this suggests that the results from the *RU* models 1, 2, 6, 8, 9, 10 as well as from the *RD* models 3, 4 are consistent. However, a firm statement of this is not possible without comparison with measurements.

A procedure of estimating the 2% exceedance values of the wave *RU* maxima and the wave *RD* maxima as well as the corresponding values of significant wave height, spectral peak period and spectral surf parameter from 1-, 10-, and 100-years return period contour lines is also demonstrated. The estimated return period values seem to be reasonable, except for the estimates based on the wave *RU* model 5 which is valid for smaller slopes than that used here. However, a firm statement of this also requires comparison with measurements.

Overall, the estimates of wave *RU* and wave *RD* are associated with a large amount of uncertainty which is partly because the wave data are from another location than the wave *RU* and wave *RD* models are based on, and partly because the models are based on data from different locations. However, the present analytical method is convenient due to its simplicity, but it should only be used for early estimates due to the uncertainties related to the results. The method should provide an appropriate and useful tool for initial estimates of wave *RU* and wave *RD* in for instance early feasibility studies and risk analysis related to the assessment of climate change effects in coastal vulnerability studies, or for estimation in the field.

## References

[1] de la Pena J M, Sanches-Gonzales J F and Diaz-Sanches R 2014 *J. of Waterways, Port, Coastal and Ocean Eng.* **140(4)** 04014015-1-04014015-11.
[2] Blenkinsopp C E et al. 2016 *Coastal Eng*. **113** 88-103.
[3] Poate T G, McCall R T and Masselink G 2016 *Coastal Eng.* **117** 176-190.
[4] Atkinson A L et al. 2017 *Coastal Eng.* **119** 15-31.
[5] Dean R G and Dalrymple R A 1984 *Prentice-Hall*, Upper Saddle River, NJ, USA.
[6] Stockdon H F et al. 2006 *Coastal Eng.* **53** 573-588.
[7] EurOtop 2018 Van der Meer J W et al., www.overtopping-manual.com.
[8] Serafin K A et al. 2019 *Coastal Eng.* **150** 1-17.
[9] Vousdoukas M I, Wziatek D and Almeida L P 2012 *Ocean Dynamics* **62** 123-137.
[10] Myrhaug D 2015 *J. of Ocean Eng. and Marine Energy* **1** 193-197.
[11] Myrhaug D and Leira B J 2017 *Coastal Eng.* **120** 75-77.
[12] Myrhaug D and Sunde T 2018 *Proc. of the Institution of Civil Engineers – Maritime Eng.* **171(1)** 40-46.
[13] Mase H 1989 *J. of Waterways, Port, Coastal and Ocean Eng*. **115(5)** 649-661.
[14] Hedges T S and Mase H 2004 *J. of Waterways, Port, Coastal and Ocean Eng.* **130(3)** 109-113.

[15] Schüttrumpf H, Bergman H and Dette H H 1994 *Proc. 24th Conf. on Coastal Eng*., Kobe, Japan, pp. 553-564.
[16] Holman R A 1986 *Coastal Eng.* **9(6)** 527-544.
[17] Divoky D and McDougal W G 2006 *Proc. 30th Conf. on Coastal Eng*., San Diego, USA, pp. 5291-5301.
[18] Bosom E and Jimenez J A 2011 *Nat. Hazards Earth Syst. Sci.* **11** 475-484.
[19] Bitner-Gregersen E M 2015 *Applied Ocean Res*. **51** 279-292.
[20] Moan T, Gao Z and Ayala-Uraga E 2005 *Marine Structures* **18(3)** 359-382.
[21] Bury K V 1975 *John Wiley & Sons*, New York, NY, USA.
[22] DNV 2014 Recommended Practice DNV- C205 Environmental Conditions and Environmental Loads. DNV GL AS.